Harnessing the Sol–Gel Process for the Assembly of Non-Silicate Mesostructured Oxide Materials

SHANNON W. BOETTCHER, JIE FAN, CHIA-KUANG TSUNG, QIHUI SHI, AND GALEN D. STUCKY*

Department of Chemistry and Biochemistry, University of California, Santa Barbara, California 93106

Received November 24, 2006

ABSTRACT

Mesostructured non-silicate oxides, with well-defined organization on the 2–50 nm size scale, may play a pivotal role in advancing vital disciplines such as catalysis, energy conversion, and biotechnology. Herein, we present selected methodologies for utilizing the sol–gel process, in conjunction with organic-directed assembly, to synthesize a variety of mesostructured oxides. The nature of the inorganic precursor is critical for this process. We discuss the development of general routes for yielding stable, nanoscopic, hydrophilic, inorganic precursors compatible with organic co-assembly. In particular, we highlight the use and characterization of organic-acid-modified transition metal oxide sol–gel precursors that allow for the synthesis and processing of designer mesostructured oxides such as titania hybrids for optical applications and porous multicomponent metal oxides useful for catalysis.

Introduction

The ability to sculpt inorganic materials in three dimensions at the nanoscale using the cooperative interactions of large amphiphilic organic molecules and soluble inorganic precursors has given birth to a large family of mesostructured materials.[1] Mesostructured materials, defined by compositional organization on the 2–50 nm size scale, have the potential to impact fields such as heterogeneous (photo)catalysis, energy, integrated optics, and biotechnology.[2,3] For example, mesostructured inorganic–organic hybrids can act as advanced optical materials due to the efficient incorporation of light-active dye molecules.[4,5] The removal of the amphiphilic organic molecules from mesostructured composites yields mesoporous materials with ultrahigh internal surface areas (often >1000 m^2/g) useful for catalysis.[6]

The history of mesostructured materials begins with zeolites, an older class of aluminosilicate framework structures with crystallographically defined subnanometer-scale organization. Zeolites are often synthesized utilizing organic templates, molecules that cocrystallize within the aluminosilicate framework.[1] Upon removal of the organic template, ordered pores commensurate in size with the template are left throughout the material. Efforts to enlarge pore sizes for catalytic applications led to the discovery that supramolecular assemblies of amphiphilic organic molecules, in contrast to isolated molecules employed for zeolite synthesis, could act as templates for larger-pore inorganic frameworks.[7,8] These micelle-forming organic molecules, termed structure-directing agents (SDAs), come in a variety of forms; ionic surfactants,[7,9] block-copolymers,[10] and even biomolecules like phospholipids[11] have been shown to template mesostructured oxides. The essential feature of SDAs is the presence of chemically bonded hydrophobic and hydrophilic components that phase segregate on the nanoscale. The hydrophobic component can solubilize organic species, while the hydrophilic component interacts with charged inorganic precursors to direct the formation of the inorganic framework. When the structure of the inorganic framework, defined by the geometry of the SDA, exhibits mesoscale (2–50 nm) periodicity, these materials are termed ordered mesostructured materials.

Herein, we describe methods for synthesizing mesostructured inorganic oxides that are not based on a silicate framework (so-called non-silicate mesostructured materials) by controlling inorganic precursor chemistry in the presence of SDAs. We briefly review the critical aspects of mesostructure synthesis derived from experiments, on both silicate and non-silicate materials. The main portion of this Account focuses on the evolution of our use of inorganic and organic acids to yield stable transition metal oxide (TMO) precursors for the synthesis of designer mesostructured oxides. Initially, this research led to the development and detailed characterization of easily processed high-index-of-refraction glasslike titania–polymer

Shannon W. Boettcher was born in Santa Cruz, CA, in 1981. He received his B.A. degree in chemistry from the University of Oregon (Eugene, OR) and began his Ph.D. work with Professor Galen Stucky at the University of California (Santa Barbara, CA) as a NSF Graduate Research Fellow in 2003. His research interests focus on the assembly of nanostructured inorganic materials, solar energy, and the physics of nanocrystalline electronic interfaces.

Jie Fan was born in Chengdu, China, in 1976. He received his bachelor's degree in chemistry from East China University of Science and Technology and his Ph.D. degree from Fudan University in July 2004, developing textural control of mesoporous silica materials under the supervision of Professor Dongyuan Zhao. In August 2004, he joined the Stucky group as a postdoctoral fellow. His research centers on the assembly of mesostructured metal oxides for applications in heterogeneous catalysis and energy conversion.

Chia-kuang (Frank) Tsung was born in Taipei, Taiwan, in 1976. He received his B.A. degree in chemistry from the National Sun Yat-Sen University in 1999 and began his Ph.D. work with Professor Stucky in 2002. His research interests focus on the nanoscale morphological control of noble metal nanoparticles and organic–inorganic hybrid materials.

Qihui Shi was born in Shanghai, China, in 1980. He received his B.S. degree in chemistry from Fudan University and began his Ph.D. work with Professor Stucky in 2003.

* To whom correspondence should be addressed. E-mail: stucky@chem.ucsb.edu. Phone: (805) 893-4872. Fax: (805) 893-4120.

Galen D. Stucky was born in McPherson, KS, in 1936. He earned his B.S. degree (1957) from McPherson College (McPherson, KS) and his Ph.D. degree with R. E. Rundle from Iowa State University (Ames, IA) in 1962. He held positions at the University of Illinois, Sandia National Laboratory, and DuPont Central Research and Development before joining the faculty of the University of California (Santa Barbara, CA) in 1985, where he is Professor in the Department of Chemistry and Biochemistry and the Materials Department. His current research interests include the synthesis and characterization of composite materials, understanding Nature's routes to organic–inorganic bio-assembly, and the chemistry associated with efficient utilization of energy resources.

10.1021/ar6000389 CCC: $37.00
Published on Web 04/27/2007

hybrids for optical applications.[5,12] Recently, this class of chemistry has enabled the synthesis of a diverse array of mesoporous multicomponent metal oxides that can also be simply processed in large quantities.[13] We conclude with several opportunities for the application of mesostructured materials in the areas of catalysis, solar energy, and biotechnology.

From Ordered Mesostructured Silicates to Transition Metal Oxides

The introduction of supramolecular templating of silicate frameworks by Mobil and Japanese scientists in the early 1990s marked the beginning of ordered mesostructured materials.[7,8] Since then, silica has been the most widely studied mesostructured material because, compared to that of the majority of inorganics, the sol–gel chemistry is simple to control. Silica-based mesostructured powders are generally synthesized from tetraethylorthosilicate (TEOS) and SDAs in either basic[7] or acidic[9,10,14] water/ethanol mixtures. The pH of this solution is critical for organic–inorganic co-assembly; reaction of the inorganic precursor with water to liberate alcohol (hydrolysis) and yield hydrophilic hydroxysilicate monomers should be fast, but the linkage of two monomers via an oxide bridge (condensation) must be slow enough for co-assembly with the SDA rather than precipitation of bulk silica or disordered composites.[15] Furthermore, the charge of soluble inorganic species, dependent on the solution pH and inorganic isoelectric point, dictates the type and degree of interactions with the SDAs.[14] Consequently, the highest-quality ordered mesoporous silicas are synthesized in either basic media (pH ~13) or acidic media (pH <2) where molecular silica species are stable and negatively or positively charged, respectively. Charged inorganic species strongly interact with charged surfactant head groups or block-copolymer hydrophilic components, either directly or through counterion and hydrogen bond-mediated pathways. These important interactions have been integrated into a generalized cooperative assembly mechanism: soluble inorganic species and surfactant molecules combine to form hybrid intermediates that are the building blocks of the final mesostructured hybrid (Figure 1).[9,14]

Non-siliceous mesostructured systems, such as transition metal oxides (TMOs), are often of greater interest than silicate mesostructures due to varied framework properties potentially useful for (photo)catalysis, sensing, optics, energy conversion, etc. However, there are two additional challenges for TMO synthesis. First, metal oxide precursors (generally chlorides or alkoxides) are much more reactive than silica-based analogues; uncontrolled condensation yields macroscopic phase segregation. Strategies for controlling the hydrolysis–condensation rates of TMO precursors include utilizing specific pH ranges, stabilizing ligands, nonaqueous media, preformed nanoclusters, controlled hydrolysis, or some combination thereof. Second, redox reactions, phase transformations, and crystallization can collapse the framework at elevated temperatures. To address this problem, block-copolymer SDAs that yield thicker inorganic walls and careful heat treatment are often employed.

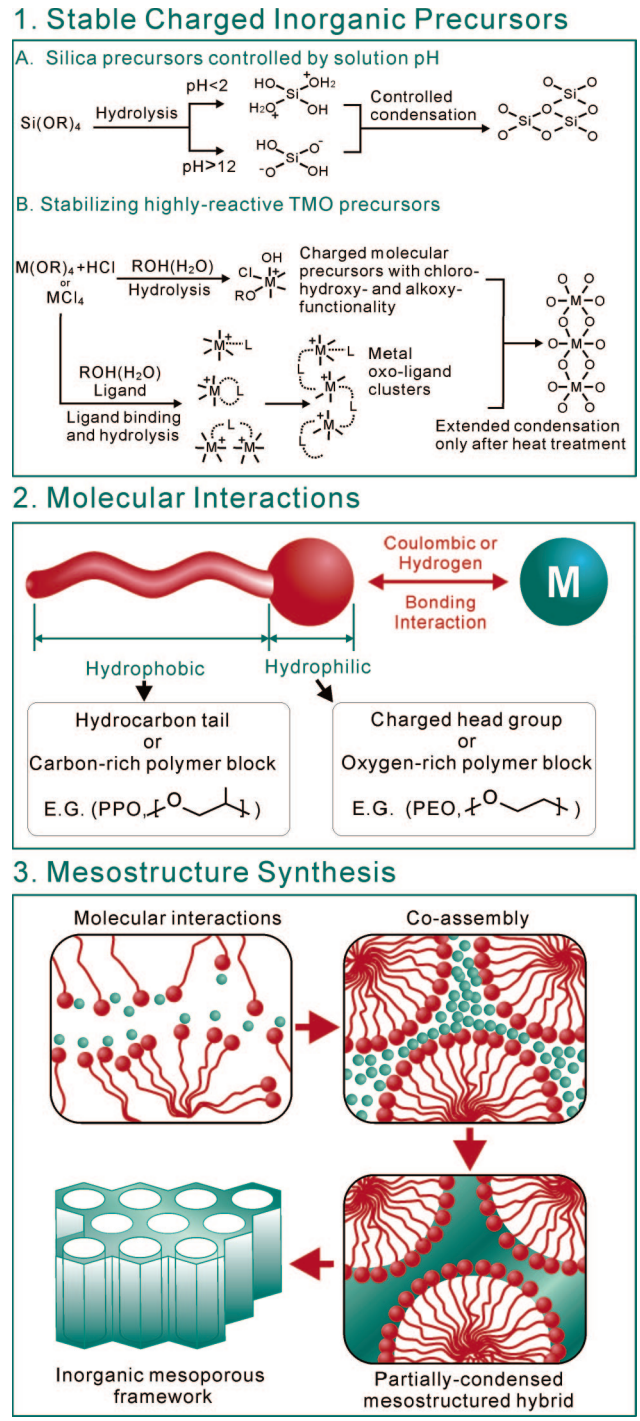

FIGURE 1. Critical aspects of sol–gel chemistry and mesostructure assembly.

The first approaches to the synthesis of TMOs were based on successful silica preparations; a series of mesostructured TMO powders were synthesized by controlling pH under aqueous conditions.[9] However, upon removal of SDA via thermal treatment, the mesoporous structures were unstable. Pinnavaia and co-workers reported a three-step assembly pathway to synthesize mesostructured alumina with crystalline walls, but the method was

restricted to alumina.[16] The next important development in the synthesis of mesoporous TMOs was the work by Ying and Antonelli, who developed a modified sol–gel route using acetylacetonate chelators.[17,18] The resulting mesostructured TiO_2 and Nb_2O_5 were thermally stable but with amorphous pore walls.

Evaporation-induced self-assembly (EISA) described by Brinker and colleagues for mesostructured silicates has proven to be an extremely useful process for both controlling macroscopic form (thin films, membranes, and monoliths) and enabling the synthesis of mesostructured TMOs.[19,20] Here, the evaporation of a volatile solvent (usually ethanol) following deposition concentrates the surfactant molecules and inorganic precursors, driving their co-assembly to form ordered mesophases. Subsequent aging, heat, or chemical treatments induce inorganic precursor condensation and lock in the mesostructure. The power of this process is twofold. First, the macroscopic morphology of the product can be tailored into application-specific geometries. Second, the co-assembly of the surfactant and inorganic precursors can be decoupled from the condensation reactions of the inorganic precursors, which is particularly useful for mesostructured TMO synthesis.

Porous TMOs with semicrystalline frameworks were realized by utilizing EISA with inorganic precursors in highly acidic alcoholic solutions.[21,22] The addition of metal chlorides to an alcohol (usually ethanol) generates HCl in situ, yielding stable chloroalkoxy precursors. The slow introduction of moisture from the ambient environment causes these precursors to partially hydrolyze. These stable, hydrophilic precursors are arranged by a block-copolymer SDA ($PEO_{20}PPO_{70}PEO_{20}$, Pluronic P123) by EISA upon dip coating. We have improved this synthesis by replacing highly reactive metal chlorides with less reactive metal alkoxides.[23] In this case, the controlled addition of aqueous hydrochloric acid (HCl) yields precursors identical to those generated in the first route. In both cases, further heat treatment locks in the mesostructure, combusts the SDA, and induces crystallite nucleation in the pore walls. The ability to crystallize the wall structure is primarily dependent on two factors. First, the use of large block-copolymer surfactants yields thick pore walls. Second, the controlled removal of water and small HCl molecules during heat-induced condensation facilitates the nanocrystal nucleation. Crystallized frameworks are important in exploiting the semiconducting properties of TMOs.[4]

Variations on this approach have been implemented by groups around the world for the synthesis of a variety of metal oxides in assorted forms.[24–27] Notably, Sanchez and co-workers have not only demonstrated that this chemistry is useful to produce thin films of a variety of mesostructured oxides, but have also worked out in detail the chemical and physical processes that transpire throughout the synthesis.[26,27] Zhao and colleagues extended this method by selecting acid–base pairs as precursors to yield multicomponent mesostructured minerals, including metal phosphates, metal borates, and mixed-valence metal oxides.[28]

Titania-Based Hybrid Optical Materials

The cooperative assembly of stabilized inorganic precursors and SDAs has made possible the design of dye-doped mesostructured hybrids for optical applications such as low-threshold waveguide microlasing.[5,12,29,30] Here, nanoscopic organic pockets, created by the SDA, selectively solubilize organic dye molecules so that they can efficiently absorb and emit light. The rigid inorganic framework provides mechanical strength and determines the average index of refraction. Such "nanocomposites" drastically outperform each of the individual components: organic dyes in inorganic hosts are poorly solubilized and form nonluminescent aggregates, whereas organic hosts have poor mechanical stability and a low index of refraction.

For optical applications, mesostructured hybrids must be easily processed into stable glasslike structures at room temperature because organic dyes degrade at elevated temperatures. This is easily achieved by utilizing silica-based hybrids because condensation occurs at room temperature under mildly acidic conditions.[29] Unfortunately, the index of refraction is limited by the low bulk index of silica ($n \sim 1.4$), which makes the fabrication of optical waveguides integrated on substrates challenging. When the framework is replaced with a material with a larger bulk index of refraction, such as titania ($n \sim 2.4$), light is more effectively confined within the waveguide structure.

We have achieved this goal by tuning the sol–gel process to fabricate stable titania-based mesostructured composite waveguides with an n of 1.6–1.7 integrated directly onto silica substrates.[5] Importantly, these materials can be formed via room-temperature processing into smooth (surface roughness of ~3 nm), optically transparent films with thicknesses ranging from hundreds of nanometers to tens of micrometers while maintaining a highly ordered mesostructure. The key to this synthetic methodology is the use of a mixture of trifluoroacetic acid (TFAA) and aqueous HCl to stabilize titania precursors in ethanolic solution with a block-copolymer SDA. We have chosen TFAA because it is a strong acid ($pK_a = 0.3$), whose carboxylate anion [trifluoroacetate (TFA)] could form strong chelating or bridging bonds to titanium species both in the precursor solution and in the final hybrid material. The controlled addition of HCl and water partially hydrolyze and charge the TFA-modified titania precursor, essential for enhancing the affinity for the hydrophilic block of the surfactant template. Without aqueous HCl, well-defined mesostructures are not obtained.

Because the chemical interactions among ligands, metal alkoxide precursors, and SDAs are critical for all modified sol–gel processes, we have characterized each step in the TFA-modified process using a series of X-ray scattering, IR/Raman spectroscopy, NMR spectroscopy, and electron microscopy experiments.[12]

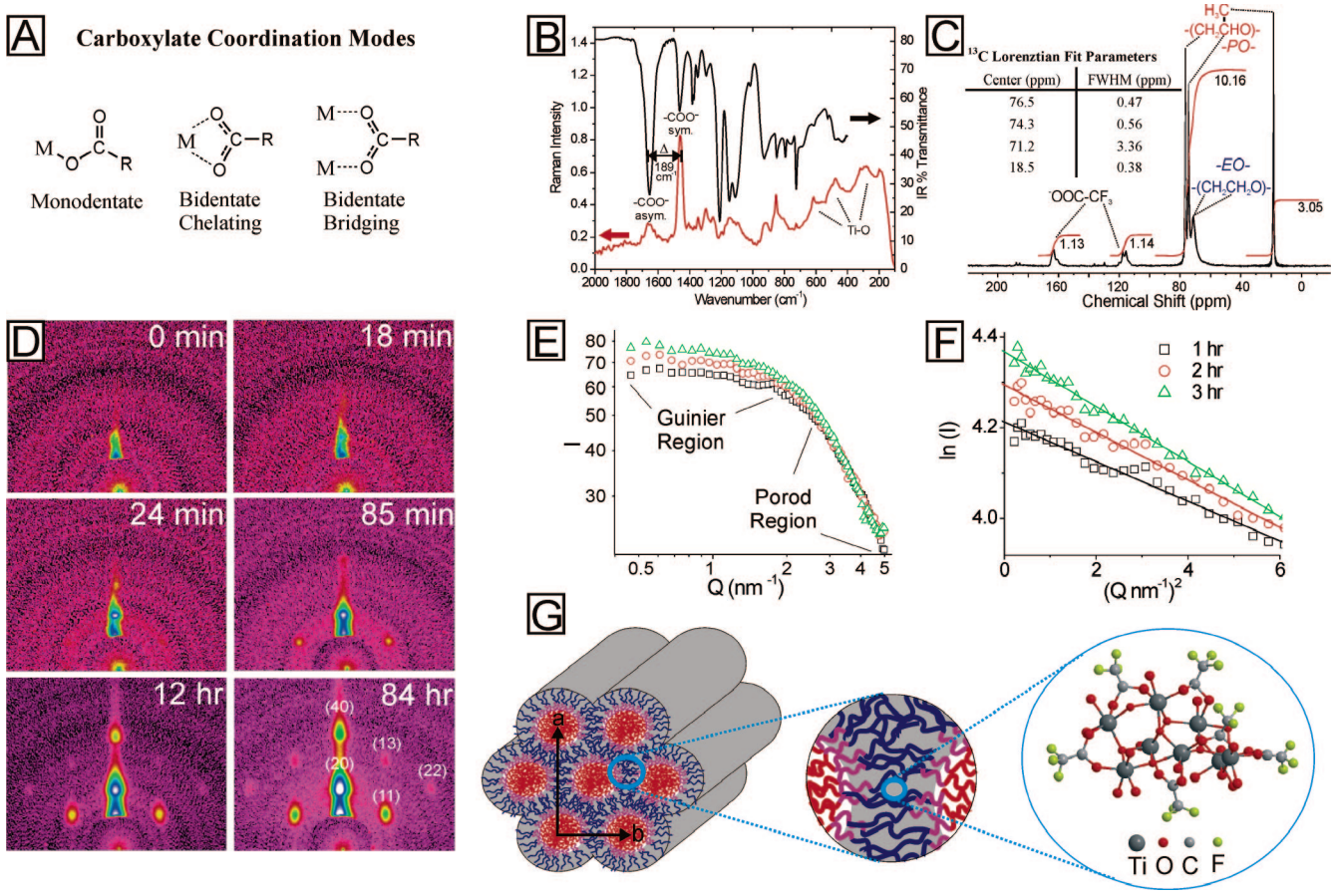

FIGURE 2. (A) Carboxylate metal ion chelating modes. (B) IR/Raman spectra of the hybrid material. TFA carboxylate stretches indicate bidentate bridging and/or chelation of the titanium center. (C) ^{13}C solid-state NMR spectrum of hybrid material. *J* coupling from the ^{19}F in the TFA is responsible for the splitting of the TFA carbon peaks. (D) In situ SAXS patterns obtained following dip coating. (E) Scattering data (log–log scale) showing typical scattering regimes for three 1 h time segments after solution preparation. (F) Linearized scattering data and the fits used to determine R_g. (G) Structural model showing hexagonal architecture due to polymer nanophase segregation between PPO cores (red) and PEO (blue) interacting with the TFA–titania framework (gray).

Inorganic Stabilization and Molecular Interactions. The bonding mode (Figure 2A) of carboxylate ligands can be identified from the difference between carboxylate asymmetric and symmetric stretching frequencies, $\Delta = \nu_{as} - \nu_{sym}$.[31,32] Generally, monodentate complexes exhibit Δ values much larger than that of the corresponding ionic structure (i.e., NaTFA). Bidentate chelating complexes exhibit Δ values significantly smaller than the ionic values, and bridging complexes have values less than, but close to, the ionic value. Analysis of the IR spectrum for the TFA–titania hybrid (Figure 2B) yields a Δ of 189 cm^{-1}, much smaller than the Δ for isolated hydrogen-bonded dimers (345 cm^{-1}) or the sodium salt (~252 cm^{-1}). This establishes that TFA binds to the titanium center in a bidentate bridging or chelating fashion. Because chelation will strain the ~120° free carboxylate O–C–O bond angle, we suspect the TFA ligands predominantly bridge adjacent titanium atoms within the hybrid material. The strength of these TFA–titania interactions is deduced from the observation that high temperatures (>400 °C) are needed to fully remove TFA. Therefore, TFA modification is unsuitable for the preparation of mesoporous materials.

It is also important for hybrid synthesis that TFAA be volatile, with a boiling point of 72.4 °C (for comparison, the nonfluorinated analogue, acetic acid, has a boiling point of 118.1 °C), so that excess TFAA evaporates along with ethanol at room temperature after structures are fabricated; IR shows free TFAA vibrations (1781 cm^{-1}) in freshly dipped films that completely disappear within 20 min of drying. Raman peaks centered from ~600 to ~280 cm^{-1} (Figure 2B) can be assigned to the Ti–O network and confirm octahedral oxygen coordination of the titanium centers.

Growth of the Modified Titania Precursor. The structure, growth, and assembly of stabilized inorganic species can be probed by small angle X-ray scattering (SAXS). The scattering intensity, $I(q)$, as a function of the scattering vector ($q = 4\pi \sin\theta/\lambda$) from the ethanolic precursor solution prepared without the structure-directing polymer (Figure 2E) exhibits typical Porod and Guinier scattering regions.[33] The low-q Guinier region, for which the approximation

$$I(q) = \Delta n_e \exp(-q^2 R_g^2/3) \qquad (1)$$

holds, is useful for analysis of particle sizes. R_g is defined as the radius of gyration of the modified titanium precursors, and Δn_e is the electron density contrast between these precursors and the ethanolic solution. A plot of the

low-q data as the natural log of intensity versus q^2 yields linear plots whose slope is R_g (Figure 2F). As the sol solution ages, R_g grows from 3.6 ± 0.1 to 4.3 ± 0.1 Å over 3 h. This size is consistent with a molecular precursor consisting of approximately four to five Ti atoms connected by oxo/hydroxo linkages and bridging TFA molecules, suitable for assembly by SDAs.

Co-Assembly of Inorganic and Organic Components. The assembly of the stabilized titania–oxoacetate oligomers into ordered nanostructures by the block-copolymer can be followed using in situ two-dimensional (2D) SAXS (Figure 2D). The X-ray beam is aligned such that it strikes the planar surface of the thin film at a grazing angle (typically <2°) as the mesostructure assembles. The scattered radiation is collected by a 2D detector. Such measurements can clarify both the kinetics of mesostructure formation and the pathways by which these processes take place.[26,34] Following dip coating, the films were immediately placed in a humidity-controlled sample chamber [relative humidity (RH) = 75%], and data collection was started. Solvent evaporation after deposition concentrates the precursor solution and induces mesophase formation.[19,20] After 30 min, the intensity of the hexagonal (11) peaks slowly grew and second-order peaks were observed after ~12 h. During the next week, the structure continued to organize, as evidenced by increasing peak intensities and the appearance of higher-order peaks. The fact that the hybrid nanostructure forms over several days suggests that TFA strongly inhibits extended condensation, even in a humid environment.

Local Structure and Interactions in the Final Hybrid Material. Once a hybrid material has been assembled, solid-state NMR is an excellent tool for analyzing local structure. Although we have performed an array of solid-state NMR experiments using three active nuclei (^{19}F, ^{1}H, and ^{13}C) to develop a model of the local structure,[12] here we present the information that can be obtained from simple ^{1}H-decoupled ^{13}C magic-angle-spinning experiments (Figure 2C). Films were scraped from glass slides and packed to fill a NMR rotor. A standard pulse sequence is used to remove the coupling of the ^{13}C nuclei to surrounding protons, and the sample is spun at 14 kHz to sharpen the resonances by averaging dipolar coupling interactions. Because the ratio of block copolymer to titanium precursor is unchanged in the final film from what was added to the precursor solution, the Ti:TFA ratio can be calculated from the ratio of polymer to TFA ^{13}C NMR signal integrations. The polymer peaks are labeled PEO for the hydrophilic polyethylene oxide block and PPO for components of the hydrophobic polypropylene oxide block. The obtained Ti:TFA ratio is 1.7:1, meaning that ~40% of the TFA added to the precursor solution remained within the composite material. TFA accounts for 50 wt % of the "inorganic network", and each pair of Ti atoms is cross-linked by at most one TFA unit.

The width of the polymer ^{13}C resonances also yields information about the interactions between the polymer blocks and the inorganic TFA–titania matrix. In general, sharp resonances correspond to nuclei with large degrees of molecular motion, whereas broad resonances indicate rigidity. Decomposition of the spectrum reveals that the PEO resonances (71.2 ppm) have a full width at half-maximum nearly an order of magnitude larger than that of the corresponding PPO resonances. The lack of a sharp component to the PEO resonance is evidence of the incorporation of the entire PEO block within the "rigid" titania–TFA matrix.

Remarks. A detailed understanding of how inorganic precursors that have been modified with organic ligands that influence their network-forming behavior and hydrophilic character interact with, and are arranged in space by the SDA hydrophillic/hydropohobic domains, is important for the design of new inorganic–organic hybrid materials. For instance, the demonstrated compatibility of modified precursors with block-copolymer assembly suggests additional functionality can be engineered into the metal oxide frameworks. Furthermore, the modification of inorganic precursors with strongly binding ligands for the preference of the formation of a "glasslike" inorganic component should be quite general and able to be extended to a variety of other inorganic precursors to enhance stability, processability, and optical quality of mesostructured hybrids.

A Modified Sol–Gel Process for Mesostructured Mixed Metal Oxides

Guided by our understanding of the chemical interactions dictating the TFA-modifed sol–gel/mesostructure co-assembly process,[12] and by early studies of acetic acid-modified titanium alkoxides for non-mesostructured sol–gel processing,[35] we have recently developed a more general sol–gel system composed of acetic acid, aqueous HCl, ethanol, and metal alkoxides (AcHE) suitable for the synthesis of non-silicate mesoporous mixed metal oxides (MMMOs).[13] Similar to the TFA ligand, nonfluorinated acetate groups bind to the metal core in a bidentate fashion, thus also controlling hydrolysis and condensation. Again, controlled quantities of HCl and water serve to partially hydrolyze and charge the modified precursor. Compared to the TFA-modified system, in which small oligomers, containing approximately four to five metal (Ti) atoms, are formed in solution, weaker-binding acetate ligands allow the growth of larger nanometer-sized inorganic precursors. Because acetate ligands are both smaller and weaker-binding, they are therefore more readily removed during heat treatment to yield mesoporous oxides. Notably, this methodology is efficient at controlling the sol–gel chemistry of many different precursors; single and/or mixed inorganic alkoxides in the AcHE solution form stable, hydrophilic nanoparticle precursors with similar sizes and growth rates, which allow for nanoparticle co-organization with amphiphilic block-copolymers into highly ordered mesostructures (Figure 3).

Controlling the Growth of MMMO Precursors. Dynamic light scattering (DLS) was employed to follow the growth of inorganic precursors in solutions exposed to the ambient environment. DLS analysis yields hydrodynamic

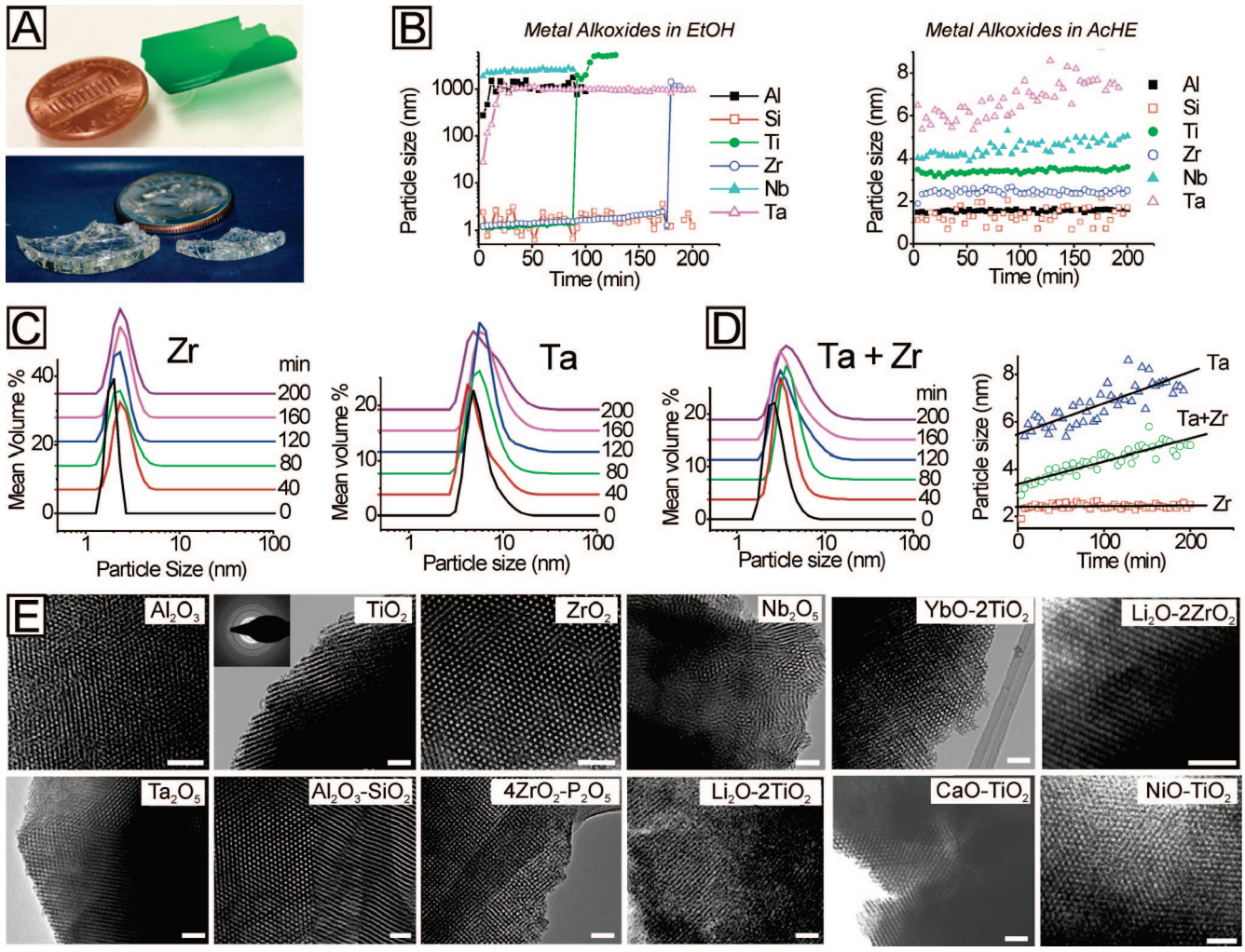

FIGURE 3. (A) Optical images of mesostructured CuO–TiO_2/Brij76 membrane (top) and PbO–TiO_2/F127 monolith (bottom). (B) Size evolution of metal alkoxides in EtOH (left) and AcHE solutions (right), both under ambient conditions. (C) Size distribution and evolution of individual metal alkoxides (Ta and Zr) and (D) their mixture in AcHE solution measured by DLS. (E) TEM images of MMMOs from the AcHE method. The scale bars are 50 nm.

particle radii that include a solvent shell. This size is larger, and generally less well-defined, than particle size descriptions from SAXS. However, DLS allows for good time resolution without the use of synchrotron X-ray sources. As expected, metal chlorides in alcoholic solution do not form clusters with diameters larger than 0.6 nm (instrumental resolution). Metal alkoxides, however, exhibit diverse condensation behaviors. $Al(OBu)_3$, $Nb(OEt)_5$, and $Ta(OEt)_5$ are highly reactive toward water with growth rates in alcoholic solution in the range of 40–500 nm/min, 4–5 order of magnitudes faster than the growth rate of $Si(OEt)_4$. Alternatively, $Ti(OBu)_4$ and $Zr(OBu)_4$ form stable nanometer-sized inorganic particles for 1–2 h under ambient conditions but then rapidly grow into macroscale precipitates (Figure 3B).

In contrast to such varied condensation behavior, metal alkoxides in the AcHE solution exhibit uniform condensation and particle-growth behavior (Figure 3B). In each case, nanosized metal–oxoacetate particles form rapidly in the AcHE solution. These nanoparticles are stable and grow slowly due to the introduction of water from the ambient environment and the esterification of acetic acid.[36] Importantly, all metal species form metal–oxoacetate particles with similar diameters in the range of 1.6–8.0 nm and normalized growth rates from 2.8×10^{-4} to 1.2×10^{-2} nm/min.

Mixed-composition nanoparticles can be fabricated in AcHE solution by simply mixing two or more metal alkoxide precursors. For example, isolated Ta and Zr species in the AcHE solution exhibit distinct particle sizes of 8.0 and 2.4 nm, respectively, but the AcHE solution containing the same total concentration of a mixture of Ta and Zr yields a single, intermediate size (5.0 nm at 200 min) and growth rate (9.7×10^{-3} nm/min) (Figure 3C,D). Such behavior is consistent with the formation of a new mixed-composition nanoparticle precursor in which the Zr and Ta are interconnected via oxo/acetate bridges. We have observed similar behavior for all the mixed metal precursor systems that have been studied, suggesting that the AcHE solution is a general route for stabilizing multicomponent oxide nanoparticle precursors that will be useful for the fabrication of multicomponent nanostructured materials.

Mesostructure Assembly and Processing. A variety of ordered MMMOs were synthesized by first combining

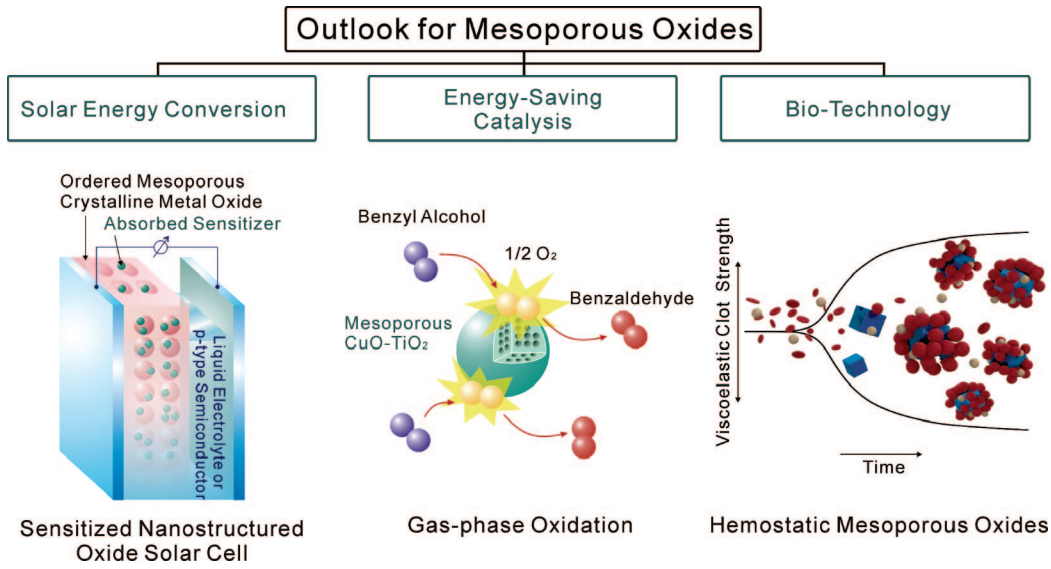

FIGURE 4. Schematic representation of the role of mesostructured oxides with controlled composition, nanostructure, and macroscopic morphology in several vital applications.

metal alkoxides with metal and/or rare earth cations (e.g., Li, Mg, Ca, Cr, Co, Ni, Cu, Yb, and Ho) and a block-copolymer SDA in the AcHE solution. Following film deposition, drop casting, or monolith molding, MMMOs were aged at 60 °C for ~24 h to remove excess acetate groups and induce limited inorganic condensation. Complete acetate and surfactant removal at 350 °C causes cell shrinkage of ~30%. Nitrogen sorption data confirm that all metal oxides have characteristics typical of mesoporous materials: uniform size distribution, high surface area, and high porosity. The high regularity of mesoporous structures in these multicomponent systems is apparent from the TEM images (Figure 3E). While many compositions yield mesostructures with amorphous frameworks, certain cases, such as TiO_2, yield semicrystalline frameworks. For catalytic applications (vide infra), the ability to introduce multiple catalytic metal oxide components into accessible wall structures may be more relevant than framework crystallization.

Remarks. There are several advantages for the preparation of mesostructured materials via AcHE solution over the conventional sol–gel process. (1) IR spectroscopy suggests that acetate groups act as bidentate ligands, which are directly bonded to the metal ions via chelating and/or bridging modes. These linkers, compared to conventional μ_i-O bridges, enhance the topological flexibility of the metal–oxoacetate frameworks, an advantage when constructing highly curved mesoscopic organic–inorganic interfaces that should allow new pore geometries. (2) The ability of acetate groups to bind and/or stabilize a range of transition and rare earth metal ions allows the synthesis of a diverse variety of MMMOs. (3) Unlike many of the related methods which are only suitable for the fabrication of thin films,[7,21,27] MMMOs synthesized via the AcHE method are easily processed into thick films, free-standing membranes, and monoliths (Figure 3A). This is important for commercial applications where large quantities of material are required, such as heterogeneous catalysis, energy storage, and nanostructured photovoltaics.

Conclusion

Harnessing the sol–gel chemistry of inorganic precursors is crucial for the synthesis of mesostructured oxides. Once stable, hydrophilic, nanometer-sized precursors are formed, a structure-directing agent can be chosen to yield the desired mesostructure. For silica-based inorganics, the chemical structure of the precursor can be simply controlled by adjusting the solution pH. The case is more difficult for non-silicate oxides where the most suitable sol–gel process depends on the desired product. For obtaining thin films with crystalline frameworks, metal chlorides in alcoholic solutions are optimal.[21,22,26,27] However, when multicomponent mesostructured metal oxides or large amounts of material are required, we find the AcHE method preferable.[13] For optical hybrid materials, strongly binding organic additives such as trifluoroacetic acid are useful in obtaining glasslike hybrids at room temperature.[12]

Outlook: Non-Silicate Mesostructured Oxides in Catalysis, Energy, and Biotechnology

Fundamental studies have revealed the synthetic aspects critical for the assembly of a wide variety of mesostructured materials. With these in mind, we conclude with selected opportunities for the synthesis and application of mesoporous oxides in the vital fields of catalysis, energy, and biotechnology (Figure 4).

Energy-Saving Catalysis. Well-defined pore sizes, tunable wall compositions and structures, large surface areas, and possibilities for internal functionalization make mesoporous oxides promising catalysts for chemical transformations.[2,6] For example, we have studied the gas-phase oxidation of benzyl alcohol to benzaldehyde over a

mesoporous CuO-TiO_2 catalyst prepared from the AcHE sol–gel system.[37] The mesoporous catalyst exhibited nearly 75% benzaldehyde conversion at 200 °C. Copper oxides loaded on zeolites or other supports exhibit less than 5% conversion under similar conditions.[38] For such applications, the ability to introduce multiple catalytic metal oxide components into accessible wall structures should allow the design of heterogeneous catalysts for a variety of chemical reactions.

Harvesting Solar Energy. Precise control over composition and three-dimensional structure at the nanometer scale using self-assembly could have a profound impact on inexpensive and efficient solar technology by ensuring that each photon is absorbed near an interface where charge separation occurs. For example, nanocrystalline metal oxide frameworks covered with a monolayer of light-absorbing dye molecules function as electron acceptors in photoelectrochemical cells,[39] and reports of such cells utilizing surfactant-templated mesoporous titania show improved performance.[40] Alternatively, solid-state solar cells can be fabricated with interpenetrating nanostructures. Mesoporous titania infiltrated with light-absorbing conjugated polymers is one example from this class of cells.[41] Another promising route may be to backfill a mesoporous semiconducting oxide with a visible-light-active semiconductor, such as CdTe or PbS, by utilizing nanoparticle precursors to fabricate all-inorganic solution-processed photovoltaics.

Each of these nanostructured photovoltaic concepts would benefit from advances in mesostructure synthesis. Ideal mesoporous oxides for nanostructured photovoltaics should have (1) large ($d \sim 20$ nm) interconnected pores that facilitate incorporation of light-absorbing material and effective hole transport, (2) a fully crystallized semiconducting wall structure to enhance electron transport, and (3) a macroscopic film structure 1–10 μm in thickness to allow for total solar absorption.

Biotechnology. Mesoporous oxides are useful in bioapplications because they can contain pores that are similar in size to, and chemically compatible with, biological macromolecules.[3] For example, we have recently investigated the activation of blood clotting by porous inorganic oxides for hemorrhage control.[42,43] It has been determined that clotting rates can be increased by utilizing highly negatively charged surfaces that accelerate protein absorption and by the codelivery of ions, such as Ca^{2+}, directly involved in the blood clotting process. Furthermore, we believe that the large surface areas of porous oxides increase the number of protein binding sites and thus also stimulate clotting. These findings should guide the design of highly effective mesoporous oxide blood-clotting agents with controlled ion release, surface charge, and pore geometries for life-saving applications.

We thank Prof. Michael Bartl, Dr. Peter Stoimenov, Martin Schierhorn, Dr. Sarah Baker, and Dr. Chengzhong Yu for valuable contributions. This material is based upon work supported by the NSF under Grant DMR-02-33728 and made use of MRL Central Facilities supported by the MRSEC Program of the NSF under Grant DMR05-20415.

References

(1) Soler-illia, G. J. D.; Sanchez, C.; Lebeau, B.; Patarin, J. Chemical Strategies to Design Textured Materials: From Microporous and Mesoporous Oxides to Nanonetworks and Hierarchical structures. *Chem. Rev.* **2002**, *102* (11), 4093–4138.
(2) Carreon, M. A.; Guliants, V. V. Ordered Meso- and Macroporous Binary and Mixed Metal Oxides. *Eur. J. Inorg. Chem.* **2005**, *1*, 27–43.
(3) Hartmann, M. Ordered Mesoporous Materials for Bioadsorption and Biocatalysis. *Chem. Mater.* **2005**, *17* (18), 4577–4593.
(4) Bartl, M. H.; Boettcher, S. W.; Frindell, K. L.; Stucky, G. D. 3-D Molecular Assembly of Function in Titania-based Composite Material Systems. *Acc. Chem. Res.* **2005**, *38* (4), 263–271.
(5) Bartl, M. H.; Boettcher, S. W.; Hu, E. L.; Stucky, G. D. Dye-activated Hybrid Organic/Inorganic Mesostructured Titania Waveguides. *J. Am. Chem. Soc.* **2004**, *126* (35), 10826–10827.
(6) Taguchi, A.; Schuth, F. Ordered Mesoporous Materials in Catalysis. *Microporous Mesoporous Mater.* **2005**, *77* (1), 1–45.
(7) Kresge, C. T.; Leonowicz, M. E.; Roth, W. J.; Vartuli, J. C.; Beck, J. S. Ordered Mesoporous Molecular-Sieves Synthesized by a Liquid-Crystal Template Mechanism. *Nature* **1992**, *359* (6397), 710–712.
(8) Yanagisawa, T.; Shimizu, T.; Kuroda, K.; Kato, C. The Preparation of Alkyltrimethylammonium-Kanemite Complexes and Their Conversion to Microporous Materials. *Bull. Chem. Soc. Jpn.* **1990**, *63* (4), 988–992.
(9) Huo, Q. S.; Margolese, D. I.; Ciesla, U.; Feng, P. Y.; Gier, T. E.; Sieger, P.; Leon, R.; Petroff, P. M.; Schuth, F.; Stucky, G. D. Generalized Synthesis of Periodic Surfactant Inorganic Composite-Materials. *Nature* **1994**, *368* (6469), 317–321.
(10) Zhao, D. Y.; Feng, J. L.; Huo, Q. S.; Melosh, N.; Fredrickson, G. H.; Chmelka, B. F.; Stucky, G. D. Triblock Copolymer Syntheses of Mesoporous Silica with Periodic 50 to 300 Angstrom Pores. *Science* **1998**, *279* (5350), 548–552.
(11) Baca, H. K.; Ashley, C.; Carnes, E.; Lopez, D.; Flemming, J.; Dunphy, D.; Singh, S.; Chen, Z.; Liu, N. G.; Fan, H. Y.; Lopez, G. P.; Brozik, S. M.; Werner-Washburne, M.; Brinker, C. J. Cell-directed Assembly of Lipid-Silica Nanostructures Providing Extended Cell Viability. *Science* **2006**, *313* (5785), 337–341.
(12) Boettcher, S. W.; Bartl, M. H.; Hu, J. G.; Stucky, G. D. Structural Analysis of Hybrid Titania-Based Mesostructured Composites. *J. Am. Chem. Soc.* **2005**, *127* (27), 9721–9730.
(13) Fan, J.; Boettcher, S.W.; Stucky, G.D. Nanoparticle Assembly of Ordered Multicomponent Mesostructured Metal Oxides via a Versatile Sol-gel Process. *Chem. Mater.* **2006**, *18*, 6391–6396.
(14) Huo, Q. S.; Margolese, D. I.; Ciesla, U.; Demuth, D. G.; Feng, P. Y.; Gier, T. E.; Sieger, P.; Firouzi, A.; Chmelka, B. F.; Schuth, F.; Stucky, G. D. Organization of Organic Molecules with Inorganic Molecular Species into Nanocomposite Biphase Arrays. *Chem. Mater.* **1994**, *6* (8), 1176–1191.
(15) Iler, R. K. *The Chemistry of Silica: Solubility, Polymerization, Colloid and Surface Properties, and Biochemistry*; Wiley: New York, 1979.
(16) Bagshaw, S. A.; Pinnavaia, T. J. Mesoporous Alumina Molecular Sieves. *Angew. Chem., Int. Ed.* **1996**, *35* (10), 1102–1105.
(17) Antonelli, D. M.; Ying, J. Y. Synthesis of a Stable Hexagonally Packed Mesoporous Niobium Oxide Molecular Sieve Through a Novel Ligand-Assisted Templating Mechanism. *Angew. Chem., Int. Ed.* **1996**, *35* (4), 426–430.
(18) Antonelli, D. M.; Ying, J. Y. Synthesis of Hexagonally Packed Mesoporous TiO_2 by a Modified Sol-Gel Method. *Angew. Chem., Int. Ed.* **1995**, *34* (18), 2014–2017.
(19) Brinker, C. J.; Lu, Y. F.; Sellinger, A.; Fan, H. Y. Evaporation-Induced Self-Assembly: Nanostructures Made Easy. *Adv. Mater.* **1999**, *11* (7), 579–585.
(20) Grosso, D.; Cagnol, F.; Soler-Illia, G. J. D. A.; Crepaldi, E. L.; Amenitsch, H.; Brunet-Bruneau, A.; Bourgeois, A.; Sanchez, C. Fundamentals of Mesostructuring Through Evaporation-Induced Self-Assembly. *Adv. Funct. Mater.* **2004**, *14* (4), 309–322.
(21) Yang, P. D.; Zhao, D. Y.; Margolese, D. I.; Chmelka, B. F.; Stucky, G. D. Generalized Syntheses of Large-Pore Mesoporous Metal Oxides with Semicrystalline Frameworks. *Nature* **1998**, *396* (6707), 152–155.
(22) Yang, P.; Zhao, D.; Margolese, D. I.; Chmelka, B. F.; Stucky, G. D. Block Copolymer Templating Syntheses of Mesoporous Metal Oxides with Large Ordering Lengths and Semicrystalline Framework. *Chem. Mater.* **1999**, *11* (10), 2813–2826.

(23) Alberius, P. C. A.; Frindell, K. L.; Hayward, R. C.; Kramer, E. J.; Stucky, G. D.; Chmelka, B. F. General Predictive Syntheses of Cubic, Hexagonal, and Lamellar Silica and Titania Mesostructured Thin Films. *Chem. Mater.* **2002**, *14* (8), 3284–3294.
(24) Brezesinski, T.; Fischer, A.; Iimura, K.; Sanchez, C.; Grosso, D.; Antonietti, M.; Smarsly, B. M. Generation of Self-Assembled 3D Mesostructured SnO_2 Thin Films with Highly Crystalline Frameworks. *Adv. Funct. Mater.* **2006**, *16* (11), 1433–1440.
(25) Choi, S. Y.; Mamak, M.; Coombs, N.; Chopra, N.; Ozin, G. A. Thermally Stable Two-Dimensional Hexagonal Mesoporous Nanocrystalline Anatase, Meso-NC-TiO_2: Bulk and Crack-free Thin Film Morphologies. *Adv. Funct. Mater.* **2004**, *14* (4), 335–344.
(26) Crepaldi, E. L.; Soler-Illia, G.; Grosso, D.; Cagnol, F.; Ribot, F.; Sanchez, C. Controlled Formation of Highly Organized Mesoporous Titania Thin Films: From Mesostructured Hybrids to Mesoporous Nanoanatase TiO_2. *J. Am. Chem. Soc.* **2003**, *125* (32), 9770–9786.
(27) Grosso, D.; Boissiere, C.; Smarsly, B.; Brezesinski, T.; Pinna, N.; Albouy, P. A.; Amenitsch, H.; Antonietti, M.; Sanchez, C. Periodically Ordered Nanoscale Islands and Mesoporous Films Composed of Nanocrystalline Multimetallic Oxides. *Nat. Mater.* **2004**, *3* (11), 787–792.
(28) Tian, B. Z.; Liu, X. Y.; Tu, B.; Yu, C. Z.; Fan, J.; Wang, L. M.; Xie, S. H.; Stucky, G. D.; Zhao, D. Y. Self-Adjusted Synthesis of Ordered Stable Mesoporous Minerals by Acid-Base Pairs. *Nat. Mater.* **2003**, *2* (3), 159–163.
(29) Yang, P. D.; Wirnsberger, G.; Huang, H. C.; Cordero, S. R.; McGehee, M. D.; Scott, B.; Deng, T.; Whitesides, G. M.; Chmelka, B. F.; Buratto, S. K.; Stucky, G. D. Mirrorless Lasing from Mesostructured Waveguides Patterned by Soft Lithography. *Science* **2000**, *287* (5452), 465–467.
(30) Scott, B. J.; Wirnsberger, G.; Stucky, G. D. Mesoporous and Mesostructured Materials for Optical Applications. *Chem. Mater.* **2001**, *13* (10), 3140–3150.
(31) Deacon, G. B.; Phillips, R. J. Relationships between the Carbon-Oxygen Stretching Frequencies of Carboxylato Complexes and the Type of Carboxylate Coordination. *Coord. Chem. Rev.* **1980**, *33* (3), 227–250.
(32) Nakamoto, K. *Infrared and Raman Spectra of Inorganic and Coordination Compounds*; Wiley: New York, 1997.
(33) Porod, G. In *Small Angle X-ray Scattering*; Glatter, O., and Kratky, O., Eds.; Academic Press: London, 1982; p 25.
(34) Doshi, D. A.; Gibaud, A.; Goletto, V.; Lu, M. C.; Gerung, H.; Ocko, B.; Han, S. M.; Brinker, C. J. Peering into the Self-Assembly of Surfactant Templated Thin-Film Silica Mesophases. *J. Am. Chem. Soc.* **2003**, *125* (38), 11646–11655.
(35) Doeuff, S.; Henry, M.; Sanchez, C.; Livage, J. Hydrolysis of Titanium Alkoxides: Modification of the Molecular Precursor by Acetic-Acid. *J. Non-Cryst. Solids* **1987**, *89* (1–2), 206–216.
(36) Schubert, U. Chemical Modification of Titanium Alkoxides for Sol-Gel Processing. *J. Mater. Chem.* **2005**, *15* (35–36), 3701–3715.
(37) Fan, J.; Zheng, N.; Stucky Galen, D. Manuscript in preparation.
(38) Genta, M.; Nishiyama, S.; Tsuruya, S.; Masai, M. Roles of Alkali-Metal Added to Cu-NaZSM-5 Catalysts in the Oxidation of Benzyl Alcohol. *J. Chem. Soc., Faraday Trans.* **1996**, *92* (7), 1267–1275.
(39) Hagfeldt, A.; Gratzel, M. Molecular Photovoltaics. *Acc. Chem. Res.* **2000**, *33* (5), 269–277.
(40) Zukalova, M.; Zukal, A.; Kavan, L.; Nazeeruddin, M. K.; Liska, P.; Gratzel, M. Organized Mesoporous TiO_2 Films Exhibiting Greatly Enhanced Performance in Dye-Sensitized Solar Cells. *Nano Lett.* **2005**, *5* (9), 1789–1792.
(41) Coakley, K. M.; McGehee, M. D. Photovoltaic Cells Made from Conjugated Polymers Infiltrated into Mesoporous Titania. *Appl. Phys. Lett.* **2003**, *83* (16), 3380–3382.
(42) Ostomel, T. A.; Shi, Q. H.; Stucky, G. D. Oxide Hemostatic Activity. *J. Am. Chem. Soc.* **2006**, *128* (26), 8384–8385.
(43) Ostomel, T. A.; Stoimenov, P. K.; Holden, P. A.; Alam, H. B.; Stucky, G. D. Host-Guest Composites for Induced Hemostasis and Therapeutic Healing in Traumatic Injuries. *J. Thromb. Thrombolysis* **2006**, *22* (1), 55–67.

AR6000389